

Probing of dielectric and ferroelectric properties of yttrium doped barium titanate ceramics

Mehraj ud Din Rather^{1*}, Rubiya Samad², Ruqiya Bhat³,

Nahida Hassan⁴, Basharat Want⁵

^{1,2,4,5}*Solid State Research Lab, Department of Physics,
University of Kashmir, Srinagar,(India)*

³*Department of Physics, University of Kashmir, Srinagar,(India)*

ABSTRACT

In this report, BaTiO₃ and Ba_{0.97}Y_{0.03}TiO₃ powders was synthesized by solid state reaction method. The XRD studies were done to ascertain the formation of tetragonal phase of pure and doped barium titanate. The microstructural analysis revealed high dense structure with uniform distribution of grains. The dielectric studies in the temperature range of 20-200 °C at different frequencies confirmed structural change from cubic to tetragonal phase. A drop in Curie temperature and decrease in dielectric loss was observed by incorporating yttrium in the BaTiO₃ lattice. The well saturated P-E hysteresis loops confirmed the ferroelectric behavior of pure and yttrium doped barium titanate. The high temperature ferroelectric studies of Ba_{0.925}Y_{0.025}TiO₃ confirmed the transition from cubic to tetragonal phase at a temperature of 117°C.

Keywords: *Dielectric, ferroelectrics, hysteresis, phase transition, yttrium*

1.INTRODUCTION

The ability of ferroelectric materials to sustain spontaneous polarization below the Curie temperature remained one of the most fascinating features of physics. From technological point of view, these form base for high dielectric constant capacitors, piezoelectric transducers, actuators, ferroelectric random access memories, electro-optic devices etc [1,2]. Besides single crystal ferroelectrics, such as Rochelle salt, where ferroelectricity arises due to hydrogen bonding [3], the polycrystalline ceramics such as BaTiO₃ is extremely important. This gained interest within the scientific community as it was first simple oxide system which displayed ferroelectricity. Due to its high dielectric constant, excellent ferroelectric and piezoelectric properties, it is extensively used in high dielectric constant capacitors, and energy storage devices. The perovskite structure of BaTiO₃ has the intrinsic capability to accommodate dopant of different size within its lattice [4, 5].The ions from the beginning of the rare earth series (La³⁺, Ce³⁺) are incorporated exclusively at the A site, whereas the

* e-mail: mehrajrather@kashmiruniversity.net

Tel: +91-9419022089

smaller ions from the end of the series (Lu^{3+} , Yb^{3+}) enter at the B site. The ions from the middle of the rare earth series, including Y^{3+} show amphoteric behavior. Apart from the dependence on the ionic radii, the ratio of incorporation at the A-site and B-site depends mainly on the A/B ratio. The Ba/Ti ratio of the starting materials seems to play a crucial role in affecting the incorporation of dopant elements into the BaTiO_3 lattice [8].

At room temperature, BaTiO_3 has perovskite structure with tetragonal symmetry, possesses a relatively high dielectric constant (~1500 - 2000). The dielectric properties of BaTiO_3 are dependent on grain size, which in turn depends upon the doping of specific ion either on A or B site [10]. Barium titanate with average grain size of $\sim 1\mu\text{m}$ exhibits dielectric constant of 3000 - 4000 at room temperature [11-13].

To optimize the electric properties, the ionic doping in ceramics is a versatile technique. The influence of rare earth dopant on the dielectric properties of barium titanate has been widely studied [14, 15]. Among various rare earths, the yttrium is the unique choice as a dopant, which tailors the dielectric and ferroelectric properties to a greater extent. In this report, the pure and yttrium doped BaTiO_3 was synthesized by solid state reaction method. Apart from microstructure, the impact of yttrium on dielectric and ferroelectric properties has been investigated in detail.

II. GROWTH AND CHARACTERIZATION

2.1 EXPERIMENTAL PROCEDURE

The pure BaTiO_3 (B1) and $\text{Ba}_{0.925}\text{Y}_{0.025}\text{TiO}_3$ (B2) samples were prepared by conventional solid state reaction method. The starting powders BaCO_3 , TiO_2 and Y_2O_3 , with purity greater than 99% were taken in required quantity. The powders were mixed for about 18 hours in an agate mortar and to attain the homogeneity, acetone was used as wet mixing agent. For the reaction to take place, the mixed powders were calcined at about 1100°C for about 3 hours with heating and cooling rate of $5^\circ\text{C}/\text{min}$. The calcined sample was then grinded for about 6 hours. The resulting sample was then pressed into pellets having 1 mm thickness and 13 mm diameter under the pressure of 10 tons by using automatic KBr press and PVA as a binder. High dense pellets were obtained by sintering them at 1350°C in alumina crucible for about 24 hours to reduce the porosity.

2.2 CHARACTERIZATION TECHNIQUES

The completion of reaction and formation of perovskite phase was confirmed by using a laboratory diffractometer with Cu K_α ($\lambda = 1.5406 \text{ \AA}$) radiation. The in-depth external morphology of the prepared samples was studied by using scanning electron microscope JEOL JSM-6390LV. The variation of dielectric constant and dielectric loss over a temperature range of $20\text{-}200^\circ\text{C}$ was studied by using Agilent 4284A precision LCR meter connected to a microprocessor based furnace fitted with a temperature controller and a specially designed two-terminal sample holder. The P-E hysteresis loops were traced by using P-E Loop Tracer, Radiant Technologies–Inc.

III.RESULTS AND DISCUSSIONS

3.1 STRUCTURAL STUDIES

Fig. 1 shows the XRD pattern of sintered disk of B2, indicating it is crystallized in tetragonal perovskite structure. All the peaks were indexed, which matches well with the Joint Committee on Powder Diffraction Standards (JCPDS) of BaTiO₃. This confirms the incorporation of Y³⁺ ions into the unit cell, maintaining the perovskite structure [16]. A slight increase in lattice constant 'a' (3.996) was observed in B2 as compared to the theoretical values for pure BaTiO₃ [17]. This increase is due to the fact that smaller Ti⁴⁺ ions are replaced by bigger Y³⁺ ions results in expansion of the unit cell [18].

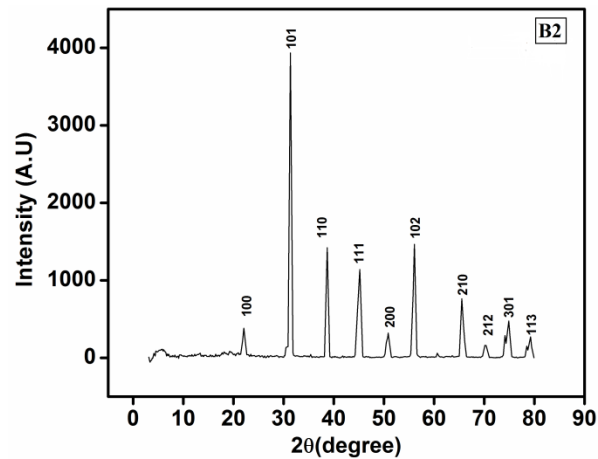


Fig. 1 X-ray diffraction pattern of B2.

3.2 MORPHOLOGICAL AND ELEMENTAL ANALYSIS

The SEM micrograph of surface at a magnification of 1500 × and field of 20 kV revealed uniform distribution of grains in both B1 and B2. The grain size was calculated by using Image J software. The decrease in grain size was observed by incorporating yttrium in the barium titanate lattice, consistent with reported one [14]. This decrease in grain size resulted in enhancement in density (4.4627 g/cm³) in B2 as compared to B1 (3.80 g/cm³). The bulk density (ρ_B) and porosity (γ) were evaluated by the following relations.

$$\rho = \frac{M}{V} \quad (1)$$

$$P = 1 - \frac{\rho_B}{\rho_T} \quad (2)$$

where M, V are ρ_T is mass, volume and X-ray densities of samples respectively.

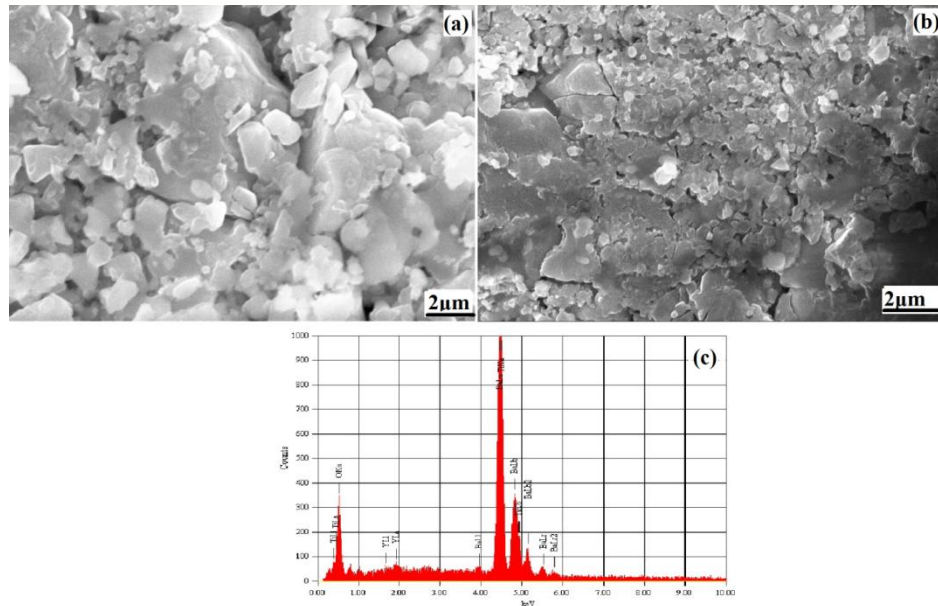


Fig. 2 (a-b) SEM micrographs of B1 and B2 (c) EDAX of B2.

Elemental analysis (EDAX) of grown B2 sample was carried out to ascertain the presence of various elements. From Fig 2 (c) it is clear that barium, titanium, oxygen and yttrium are present in the sample B2.

3.3 DIELECTRIC STUDIES

Fig. 3 shows the temperature dependence of dielectric constant (ϵ') for B2 ceramic at different frequencies. The dielectric constant has been found to increase gradually to a maximum value with increase in temperature and then decreases. This confirms a phase transition from low temperature tetragonal phase to high temperature cubic phase. All the peaks are broadened, confirming diffused phase transition. The broadness of the peak is an indication of the disorder existing on the B-site position [19]. The maximum values of dielectric constant at the Curie temperature are tabulated in Table II. The variation of ϵ' with temperature for B1 at a selected frequency of 100 Hz is shown in inset of Fig. 3. In sample B2, the increase in dielectric constant is observed as compared to B1. The increase in ϵ' is attributed to enhanced grain-growth and dense microstructure, consistent with SEM results. Also with the incorporation of yttrium in barium titanate lattice, the Curie temperature was reduced from 123 to 117 °C. This drop in Curie temperature is also due to decrease in grain size [20].

The variation of dielectric loss ($\tan\delta$) with temperature for B2 sample is shown in Fig 4, with inset showing corresponding variations for B1 sample. The $\tan\delta$ shows variation similar as that of ϵ' supporting ferroelectric transition. In comparison to B1, the $\tan\delta$ of B2 ceramic is reduced. This decrease is due to reduction in number of mobile charge carriers by yttrium doping [15]. The $\tan\delta$ value of B2 near Curie temperature is small (0.16), as compared to that of B1 (0.19). The low values of $\tan\delta$ make such ceramic materials valuable for technological applications.

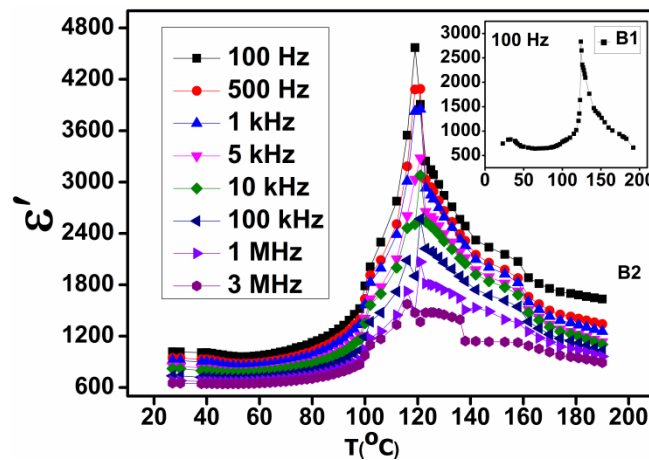


Fig. 3. Variation of dielectric constant (ϵ') with temperature for B2, with inset showing corresponding variations for B1.

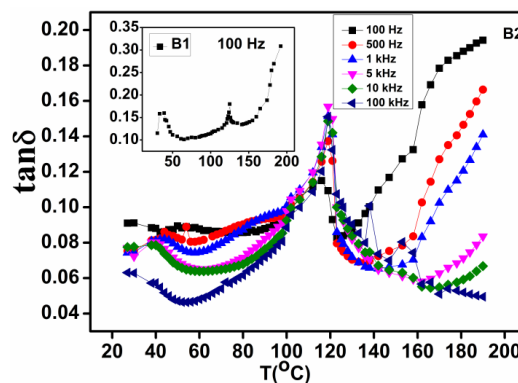


Fig.4. Variation of dielectric loss ($\tan\delta$) with temperature for B2, with inset showing corresponding variations for B1.

3.4 FERROELECTRIC STUDIES

The polarization–electric field (P–E) hysteresis loops were traced in order to ascertain the ferroelectric behavior of the B1 as well as B2 samples. At room temperature (RT), B1 shows hysteresis loop with high value of saturation polarization (P_s) as compared to B2, as depicted in Fig. 5. Also the various electric parameters like coercivity and remnant polarization are reduced due to yttrium doping. This is attributed to the fact that ferroelectric properties are affected by the composition, microstructure and lattice defects, such as oxygen vacancies created in these materials by yttrium doping [21-23]. In soft ferroelectrics, with higher-valent substituent's, the defects are cation vacancies. These cationic vacancies tend to form dipolar defects and the random field created due to these dipolar defects lowers the activation barrier required for nucleation of new domains, leading to lower E_c [24,25]. With the increase in temperature for B2, all the electric parameters are reduced. At the higher temperature of 117°C, the P-E hysteresis changed into a straight line confirming ferroelectric transition from ferroelectric to paraelectric state.

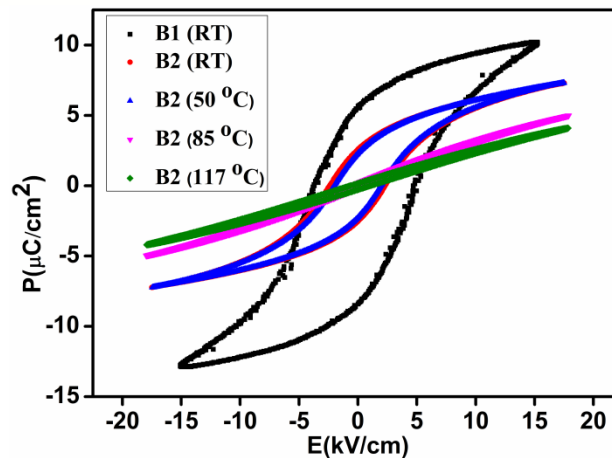


Fig. 5. P-E hysteresis of B1 at room temperature and that of B2 at different temperatures

IV.CONCLUSIONS

The XRD studies confirmed tetragonal phase of yttrium doped barium titanate, confirming yttrium is incorporated in the barium titanate. The microstructural analysis revealed high dense structures. The dielectric studies confirmed structural change from cubic to tetragonal phase. A drop in Curie temperature and decrease in dielectric loss was observed by substituting yttrium in the BaTiO₃ lattice. The ferroelectric studies confirmed reduction of ferroelectric parameters by yttrium doping in barium titanate. The temperature dependent ferroelectric studies of Ba_{0.925}Y_{0.025}TiO₃ confirmed the transition from tetragonal to cubic phase at a temperature of 117°C, where P-E loop was reduced to a straight line.

REFERENCES

- [1] L. L. Hench, J. K. West, (Principles of Electronic Ceramics, Wiley, New York 1990).
- [2] Setter, Nava, and E. L. Colla, (Ferroelectric ceramics: tutorial reviews, theory, processing, and applications. Birkhauser, 1993).
- [3] B. Want, and R. Samad, *Journal of materials scienc*, **49 (14)**, 2014, 4891-4898.
- [4] D. Makovec, S. Zoran, and D. Miha, *Journal of the American Ceramic Society*, **87(7)**, 2004 1324-1329.
- [5] M. D. Glinchuk, P. B. Igor, M. K. Sergei, V. L. Valentin, M. S. Alla, B. G. Anatolii, I. V. Oleg, and Z. Y. Yanchevskii, *Journal of Materials Chemistry*; **10(4)**, 2000, 941-947.
- [8] J. Zhi, A. Chen, Y. Zhi, P. M. Vilarinho, and J. L. Baptista, *Journal of the American Ceramic Society*, **82(5)**, 1999, 1345-1348.
- [10] K. Kinoshinta, A. Yamaji, *J. Appl. Phys.*; **47 (I)**, 1976, 371-374.
- [11] M. Rubayyat, M. S. Hossain, and M. F. Islam, *Materials Engineering-Materiálové inžinierstvo (MEMI)*, **20(1)**, 2013, 45-53.
- [12] A. S. Shaikh, R. W. Vest, G. M. Vest:In: IEEE 6th Int. Svmp. App. Ferroelectr.,Ed.: Van E. Wood, Bethlehem PA, 1986, pp. 126-129.

- [13] G. H. Jonkkr , W. Noorland: In.: Science of Ceramics 1, Ed.: G. H. Stewart. Academic Press London, London, 1962, pp. 255-264.
- [14] Piyush Kumar Patel, K.L. Yadav, *Physica B*, **442**, 2014, 39–43.
- [15] D. Shana , Y.F. Qua, J.J. Songb, *Solid State Communications*, **141**, 2007, 65–68.
- [16] S. Bhaskar Reddy, M.S. Ramachandra Rao, and K. Prasad Rao, *Appl. Phys. Lett.*, **91**, 2007, 022917.
- [17] M. Fechner, S. Ostanin, and I. Mertig, *Phys. Rev. B*; **77**, 2008, 094112.
- [18] P. Ren, Q. Wang, X. Wang, L. Wang, J. Wang, H. Fan, and G. Zhao, *Mater. Lett.*, **174**, 2016, 197.
- [19] A. Munpakdee, K. Pengpat, J.Tontrakoon,T.Tunkasiri, *Smart Mater.Struct.*, **15**, 2006, 1255.
- [20] S. BhaskarReddy, M.S.Ramachandra Rao, K. Prasad Rao, *Appl.Phys.Lett.*, **91**, 2007, 022917.
- [21] H. Watanabe, T. Mihara, H. Yoshimori and C. A. paz. De Arauja, *Jpn, J. Appl. Phys.*, **34**, 1995, 5240.
- [22] Wei Wang, Jun Zhu, Xiang Yu Mao, Xiao-Bing Chen, *Materials Research Bulletin*, **42**, 2007, 274- 280.
- [23] M. Miyayama, T. Nagamoto and O. Omoto, *Thin Solid Films*, **300**, 1997, 299.
- [24] Y. Noguchi, M. Miyayama, K. Oikawa, T. Kamiyama, M. Osada and M. kakahana, *Jpn. J. Appl. Phys.*, **41**, 2002, 7062.
- [25] W. Wang, J, Zhu, X. Y. Mao and X. B. Chen, *Mater. Res. Bull.*, **42**, 2007, 274.